ARTICLE

OBC
www.rsc.org/obc

# L-Tartaric acid assisted binary organogel system: strongly enhanced fluorescence induced by supramolecular assembly

**Chunyan Bao, Ran Lu,* Ming Jin, Pengchong Xue, Changhui Tan, Guofa Liu and Yingying Zhao**

*College of Chemistry, Jilin University, 2519 Jiefang Road, Changchun, 130023, P. R. China. E-mail: luran@mail.jlu.edu.cn*

***Received 11th April 2005, Accepted 27th April 2005***
***First published as an Advance Article on the web 11th May 2005***

A new series of binary organogels, which showed good gelated capability and strongly enhanced fluorescence emission, were designed and prepared by simply mixing two components of L-tartaric acid and alkoxyl substituted stilbazoles. It was found that L-tartaric acid could not only introduce stilbazole with fluorescent property into the gel system, but also provided a main motif for the formation of the gel-phase *via* multiple hydrogen bonds. Meanwhile, π–π interactions between the complexes also played a key role in the gel formation. The decreased nonradiative process, suggested by the longer fluorescent lifetime of aggregates than that of monomers and the presence of the J-aggregation for the aggregated state, favored the enhanced fluorescence emission.

## Introduction

Gels derived from low molecular mass compounds have attracted considerable interest in recent years on account of their unique features and potential applications for new soft organic materials,[1] template synthesis,[2] drug delivery,[3] separations and biomimetics.[4] Compounds with various structural diversities have been reported to gelatinize organic liquids efficiently, such as the derivatives of carbohydrates,[5–7] amino acids,[8–9] urea[10–11] and cholesterol.[12–15] Recently, there has been increasing interest in the development of the functional gel systems with π-conjugated molecular structures due to their potential applications in various optoelectronic fields, including enhanced charge transport, fluorescence and sensing abilities.[16] However, it was often difficult to introduce the desired functional groups into the individual building blocks for the gel systems. It is believed that binary gel systems may assist to introduce the functional groups and obtain organogelators with functionalities in a facile way, in which the two components may interact with each other to obtain a complex by electrostatic action,[17] hydrogen bonding,[18] donor–acceptor interactions[19] and metal coordination,[20] then further self-assemble *via* intercomplex interactions, *e.g.* hydrogen bonding, π-π interactions or Van der Waal's forces, to form the fully gelated network. Until now, limited two-component gelators had been reported.

In this paper, we report the design of a series of binary gel systems comprised of L-tartaric acid and 4-(4-alkoxybenzoyloxy)-4′-stilbazole (nSZ) derivatives, in which the alkyl chain substituted stilbazoles have been shown to be versatile materials for the construction of molecular materials, including optically nonlinear systems, pyroelectric Langmuir–Blodgett fabrications and metallomesogens,[21] but they generally cannot self-assemble into supramolecular gels by themselves. As known, L-tartaric acid is a good proton donor which can interact with stilbazoles *via* multiple hydrogen bonds to access the self-assembly.[22] Herein, excellent transparent gels can be formed based on the hydrogen bonded complex derived from L-tartaric acid and stilbazoles. Interestingly, such binary gels showed good gel capability and unusually enhanced fluorescence, which is novel and very significant for functional gel materials.

## Results and discussion

The complexes (**I–III**) of the two-component gelators as shown in Scheme 1 were prepared from L-tartaric acid and two eq. of the corresponding 4-(4-alkoxybenzoyloxy)-4′-stilbazoles (nSZ) in THF. The formation of the intermolecular hydrogen bonds between nSZ and L-tartaric acid in the complexes can be confirmed by FT–IR spectroscopy due to the appearance of two broad peaks at *ca.* 2450 $cm^{-1}$ and 1930 $cm^{-1}$.[23] Neither nSZ nor L-tartaric acid alone is capable of gelating the solvents, while the complexes can gel most chlorinated solvents including chloroform, dichloromethane, dichloroethane, chlorobenzene and 1,3-dichloropropane. In dichloromethane, for example, the complexes are insoluble at rt, but turn into a clear solution by heating to 40 °C in a capped vial and, upon cooling to rt, an immobilized transparent gel is readily formed within several hours at contents as low as 0.3 wt% (w/v). During the preparation of sols, gels and xerogels of complexes (**I–III**), it was noticed that their colour changes sensitively. They are almost colorless in the solid-phase or in nonchlorinated solvents, but when the complexes were added into the chlorinated solvents the mixture turned light yellowish–green and the gels obtained showed a yellowish–green colour. To reveal the origin of the colour changes and the formation of the gel, the optical and structural properties of the complexes in the monomer state and in the gel-phase were examined.

To obtain a visual image for the assemblies of the complexes, the scanning electron microscope (SEM) pictures of the dichloromethane gels were measured, as shown in Fig. 1. The SEM picture of complex **II** showed a three-dimensional network consisting of ribbons with largely knotted nodes (connected spots), which suggested that the gel constituted by a robust gel system with permanent solid-like networks. Furthermore, the SEM picture for complex **I**, with a shorter alkyl chain in the stilbazole unit, was filled with more or less straight ribbons, whereas that of complex **II** was filled with frizzy ribbons. On the other hand, the xerogel of complex **III** resulted in a sheet-like structure. It was assumed, therefore, that the complexes with an alkyl chain shorter or longer than that of complex **II** (n = 10) tended to aggregate into two-dimensional morphologies.

In order to ascertain how the complex aggregated into a supramolecular structure, both FT–IR and UV–vis investigations were performed. From FT–IR absorption data, as shown in Table 1, it was found that the OH absorption in the xerogel state shifted to shorter wave-numbers and split into two peaks. The absorption of C=O also shifted to lower wave-numbers compared with the complexes before gelation, which showed that the hydrogen bonds did indeed take place between the OH and C=O in the intermolecular L-tartaric

DOI: 10.1039/b504945h

 

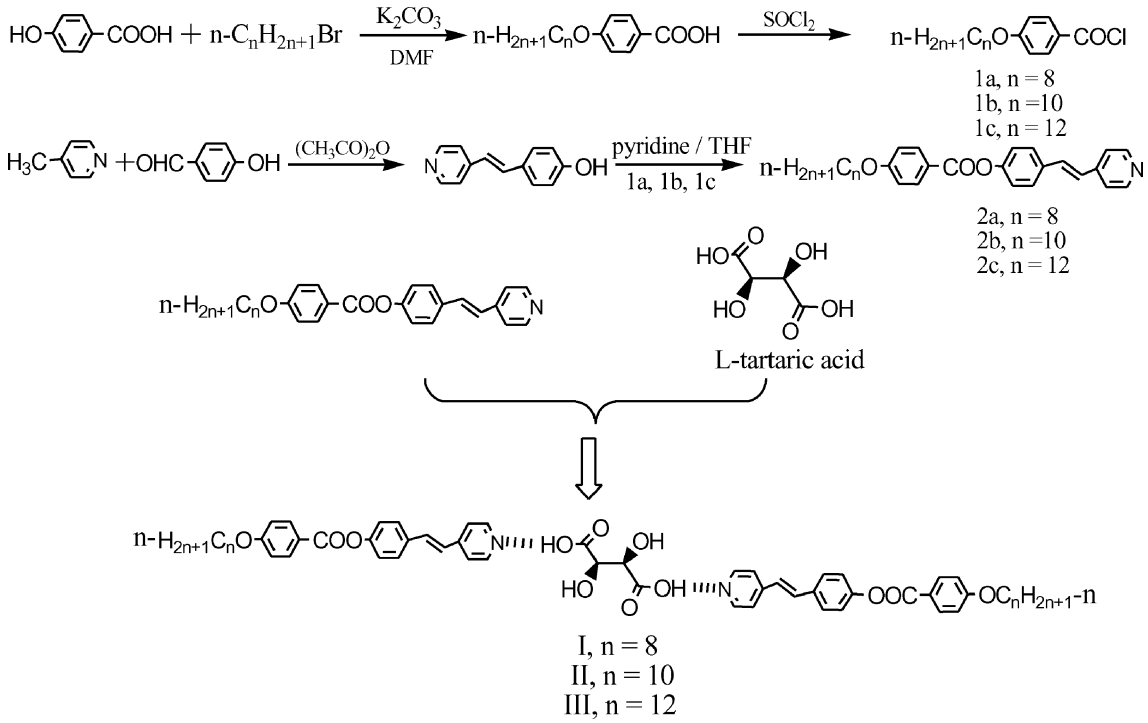


**Scheme 1** The synthetic routes for complexes **I–III**.

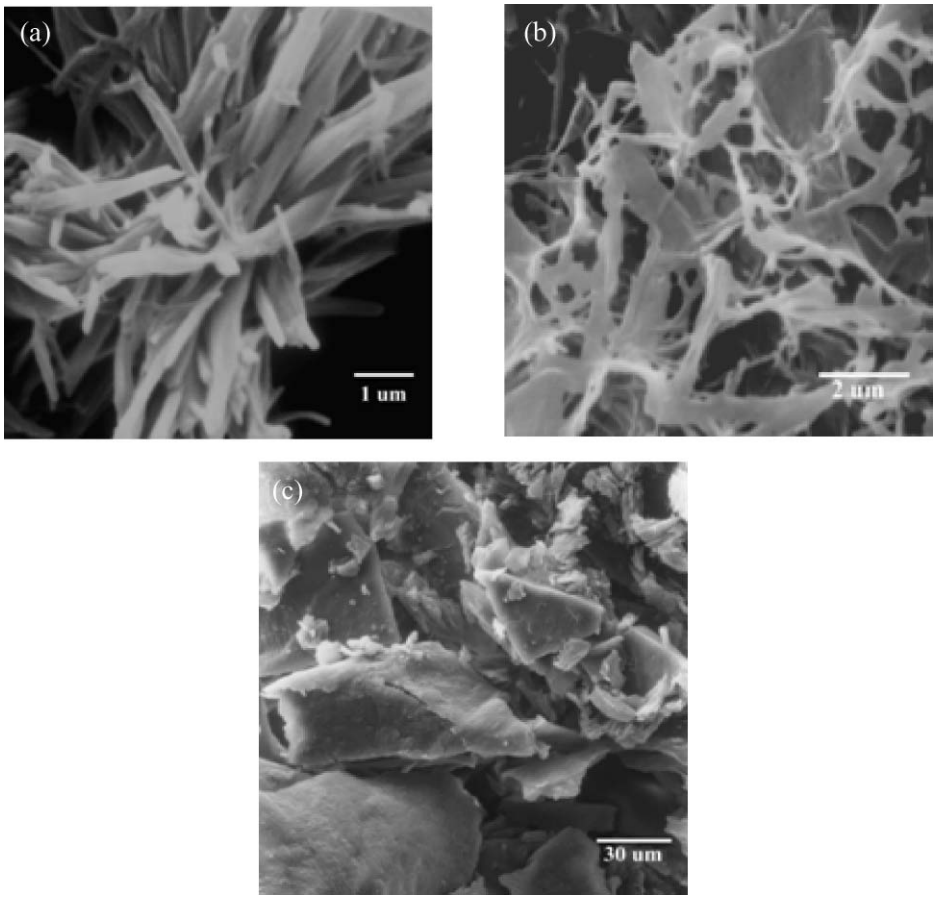


**Fig. 1** The SEM pictures of the xerogels obtained from 0.3 wt% dichloromethane gels: (a) n = 8; (b) n = 10; (c) n = 12.

acid (hydrogen bonding b, as shown in Scheme 2) during the formation of the organized superstructure.[24] In addition, and as mentioned above, the appearance of two broad peaks at *ca.* 2450 and 1930 $cm^{-1}$ confirmed another kind of hydrogen bonding (hydrogen bonding a, as shown in Scheme 2) formed between nSZ and L-tartaric. Therefore, the hydrogen bonding not only introduced the functional stilbazole groups into the gels, but also helped the formation of supramolecular aggregations, which could be further proved by the below experiment. It was found that one small additional drop of methanol could completely destroy the gel in solution, in which the hydrogen bonding between the pyridine in the nSZ and the carboxyl in the L-tartaric

**Table 1** FT–IR absorption data for A, nSZ; B, hydrogen bonding complexes before the gelation; and C, xerogels of the complexes

| Number of alkyl chains | | OH/cm$^{-1}$ | $\nu_{as}(CH_2)$/cm$^{-1}$ | $\nu_s(CH_2)$/cm$^{-1}$ | Hydrogen bonds of kind a in the complexes/cm$^{-1}$ | C=O/cm$^{-1}$ |
|---|---|---|---|---|---|---|
| n = 8 | A | | 2915.2 | 2850.6 | | 1721.9 |
| | B | 3422.9 | 2923.8 | 2853.9 | 2452.3, 1916.8 | 1730.9 |
| | C | 3264.3, 3128.4 | 2922.8 | 2852.7 | 2552.2, 1921.6 | 1724.9 |
| n = 10 | A | | 2915.1 | 2849.2 | | 1722.1 |
| | B | 3412.7 | 2921.0 | 2852.3 | 2431.5, 1913.9 | 1728.3 |
| | C | 3278.5, 3131.2 | 2919.2 | 2851.5 | 2559.9, 1938.5 | 1721.7 |
| n = 12 | A | | 2915.2 | 2848.8 | | 1721.8 |
| | B | 3435.3 | 2922.2 | 2851.1 | 2431.5, 1933.4 | 1729.8 |
| | C | 3277.1, 3135.6 | 2917.2 | 2850.6 | 2543.2, 1950.2 | 1722.0 |

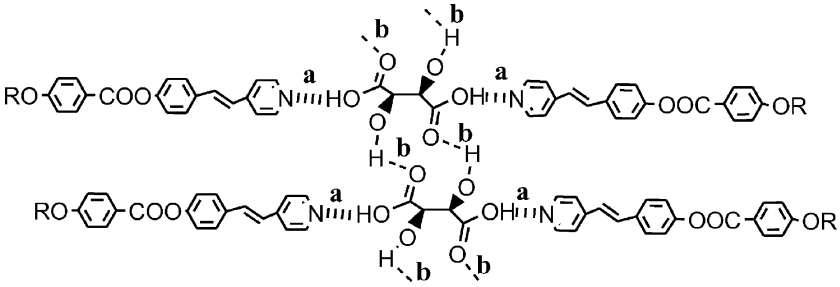


**Scheme 2** Schematic illustration for the structure of the complexes and the possible self-assembled mode of the complexes in the gel-phase.

acid were still maintained, due to the FT–IR data being similar to those of the samples without treatment with $CH_3OH$. It was suggested that the hydrogen bonding aggregations were broken into the monomer state and intermolecular hydrogen bonds between the OH and C=O (hydrogen bonding b) in the intermolecular L-tartaric acid were the key motif for gel formation.

The UV–vis absorption spectra for the gel in dichloromethane were measured and compared with the corresponding monomer in cosolvent (40 μM in $CH_2Cl_2$–$CH_3OH$ = 9 : 1 by volume). For example (as seen in Fig. 2), for the series of n = 10, the peak assignable to stilbazole gave a broadened and red-shifted band in the gel-phase, which was quite different from that of the monomer state of the complex, which illustrated the formation of J-aggregation within the gel. Therefore, it was suggested that the π–π interaction also played a key role on the formation of the binary gels. Based on the above results, the aggregated mode could be suggested to be as is shown in Scheme 2.

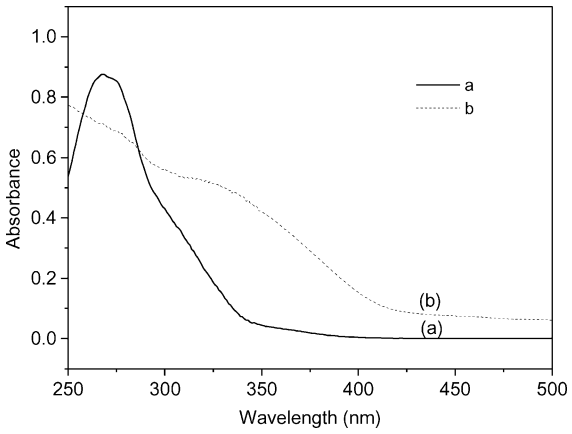


**Fig. 2** UV–vis absorption spectra for the series of n = 10: (a) the monomer state of complex **II** in mixed solvents $CH_2Cl_2$–$CH_3OH$ = 9 : 1 by volume; (b) the gel state in dichloromethane.

Significantly, a remarkable fluorescence enhancement induced by self-assembly of the complexes was found (see Fig. 3a). When excited at 365 nm (using the series of n = 10 as the example), the fluorescence intensity for the complex in the $CH_2Cl_2$ gel-phase (the right side of Fig. 3b) was almost 1000 times stronger

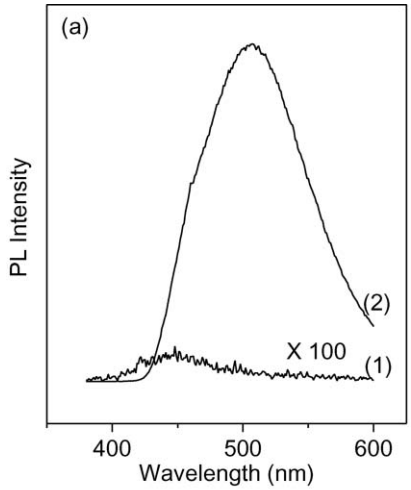


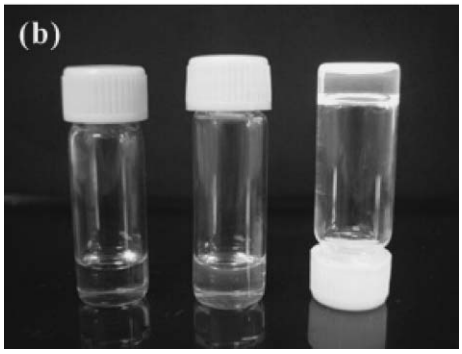


**Fig. 3** (a) Fluorescence spectra of complex **II** (1) in $CH_2Cl_2$–$CH_3OH$ = 9 : 1 solution at 0.3 wt% (w/v) and (2) in $CH_2Cl_2$ gel at 0.3 wt%. (b) Fluorescence images of $CH_2Cl_2$–$CH_3OH$ = 9 : 1 solution (9/1) at 0.3 wt% (left), $CH_2Cl_2$ solution at 40 μM (center) and $CH_2Cl_2$ gel at 0.3 wt% (right) under 365 nm illumination.

than that of the nonfluorescent monomer (the left side of Fig. 3b) under the same concentration of 0.3 wt %. To the best of our knowledge, this is the highest fluorescence modulation among the previous organogel systems for showing fluorescent enhancement.[25] Furthermore, the red-shift of the fluorescence maxima of the gel compared with the monomer state was based on the stabilization effect of aggregation in the excited

state, which matched the UV–vis absorption results. The dilute solution in 40 μM $CH_2Cl_2$ also showed the yellowish–green luminescence similar to the luminescence of the gel in $CH_2Cl_2$, which suggested that the complex had already self-assembled into H-bonded aggregates even in the dilute solution. This was also confirmed by the IR absorption data being similar to those of the gel. Generally, the enhanced emission is always attributed to the combined effects of molecular planarization, restricted molecules motions and J-aggregation formation.[26] Here, considering the maximum absorption of the aggregated complexes gives only one bathochromic shift, the molecular planarization does not happen. Based on the UV–vis spectra, the J-aggregations were formed in the self-assemblies and the molecules arranged into a slanted stack and the transition to the lower couple excited state of the molecules was allowed, which favored the enhancement of the emission.[27] When the hydrogen bonded aggregates formed, the interactions between the molecules confined the rotation of the groups in the molecules. Therefore, the synergetic effect of the limited molecular motions and the formation of the J-aggregation induced the enhancement of the fluorescence emission. This significant enhanced emission may be useful for some sensors, such as an on/off fluorescent switch which is sensitive to temperature.

To obtain further information on the nature of the excited state, a nanosecond time-resolved fluorescence was examined. The emission decay profiles were monitored in 450 nm for the monomer state solution (40 μM in $CH_2Cl_2$–$CH_3OH$ system) and 500 nm for aggregated state solution in 40 μM $CH_2Cl_2$. As shown in Fig. 4, the monomer solution gave a short lifetime of 1.2 ns and the aggregated state solution under the same concentration showed a long lifetime of 3.5 ns. It implies that the formation of aggregation restricts the rotation and vibration of the groups in the molecules, so that longer emission lifetimes were dectected.[16a,26] The limited molecular motions led to the a decreasing of the nonradiative relaxation process, which led to the enhanced fluorescence emission effectively.

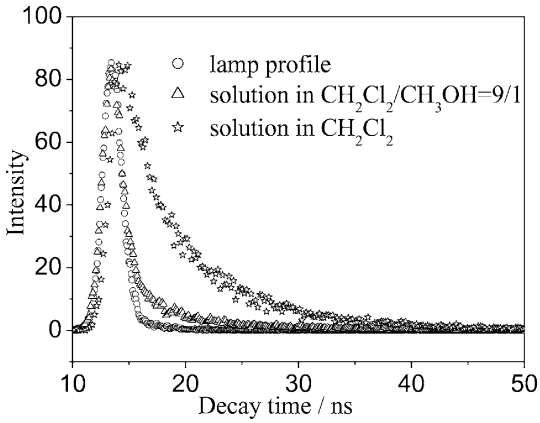


**Fig. 4** The fluorescence decay profiles of complex **II** for monomer (△) in 40 μM cosolvent $CH_2Cl_2$–$CH_3OH$ = 9/1 and H-bonded aggregate (☆) state in 40 μM $CH_2Cl_2$ solution. The samples were excited at 365 nm and monitored at 450 nm and 500 nm respectively.

## Conclusions

A series of functional binary gels with good gelated capability based on L-tartaric acid and stilbazoles were prepared and showed good gelated capability in most chlorinated solvents. Herein, L-tartaric acid not only introduced the functional groups (fluorescent stilbazole group) into the gel system, but also provided a main motif for the formation of the gel-phase *via* multiple hydrogen bonds, which provide a simple and more extensive way for the fabrication of functional gels through non-covalent interactions. The obtained gels showed strongly enhanced emission and a longer lifetime due to the supramolecular self-assembling. It is hoped that such fluorescence modulated organogels may be useful for some sensors. In addition, it provides an extensive way to prepare functional gels *via* non-covalent interactions.

## Experimental

### Measurements

$^1$H NMR spectra were determined with JEOL JNM-500EX. UV–visible absorption spectra were recorded with a Shimadzu UV-2201 UV–visible spectrophotometer. Fourier transform infrared (FT–IR) spectra were measured at rt on a Nicolet Impact 410 FT-IR spectrometer. Scanning electron microscopy (SEM) was taken with a Japan Hitachi model X-650 San electron microscope. Fluorescence spectra were recorded on a Shimadzu RF-5301 Luminescence Spectrometer. Fluorescence lifetimes were measured using the time correlated single photon counting technique with FL920-fluorescence lifetime spectrometer. The excitation source was a nF900 nanosecond flashlamp. Lifetimes were obtained by deconvolution of the decay curves.

### Materials

All the materials were used as received and the solvents were dried and distilled prior to use. The alkoxybenzoyl chlorides were prepared according to a general procedure and were used without any further distillation.

**4-(4-Octyloxybenzoyloxy)-4′-stilbazole (8SZ).** 4-Hydroxy-4′-stilbazole (3.0 g, 15.2 mmol) was dissolved in dry pyridine (100 ml) and a solution of 4-octyloxybenzoyl chrolide (17.3 mmol) in dry THF (20 ml) was added dropwise to the pyridine solution within 30 min at rt. After the mixture had been stirred overninght, most of the THF and pyridine was distilled off. The residue was poured into a large amount of water, the precipitate was filtered and recrystallized twice from ethanol and twice from cyclohexane. Yield 80%. Elemental analysis calculated for $C_{28}H_{31}NO_3$: C, 78.30; H, 7.22; N, 3.26%. Found: C, 78.04, H, 7.35; N, 3.23%. FT–IR ($cm^{-1}$): 2915.3, 2850.7, 1721.9, 1609.4, 1592.3, 1511.8. $^1$H NMR ($CDCl_3$, 300 MHz): 8.597 (2H, s, PyH), 8.145 (2H, d, ArH), 7.600 (2H, d, ArH), 7.360 (2H, d, PyH), 7.304 (1H, s, CH=CH), 7.234 (2H, d, ArH), 7.027 (1H, s, CH=CH), 6.968 (2H, d, ArH), 4.048 (2H, t, $CH_2$), 1.300–1.851 (12H, m, $CH_2$), 0.896 (3H, t, $CH_3$).

**4-(4-Decyloxybenzoyloxy)-4′-stilbazole (10SZ).** This compound was prepared in a similar way to **8**SZ. Yield 82%. Elemental analysis calculated for $C_{30}H_{35}NO_3$: C, 78.52; H, 7.50; N, 3.16%. Found: C, 78.57, H, 7.78; N, 3.27%. FT–IR ($cm^{-1}$): 2915.1, 2849.2, 1722.1, 1609.3, 1592.6, 1511.8. $^1$H NMR ($CDCl_3$, 300 MHz): 8.599 (2H, s, PyH), 8.150 (2H, d, ArH), 7.590 (2H, d, ArH), 7.391 (2H, d, PyH), 7.356 (1H, s, CH=CH), 7.234 (2H, d, ArH), 7.028 (1H, s, CH=CH), 6.972 (2H, d, ArH), 4.049 (2H, t, $CH_2$), 1.284–1.851 (16H, m, $CH_2$), 0.889 (3H, t, $CH_3$).

**4-(4-Dodecyloxybenzoyloxy)-4′-stilbazole (12SZ).** This compound was prepared in a similar way to **8**SZ. Yield 75%. Elemental analysis calculated for $C_{32}H_{39}NO_3$: C, 79.14; H, 8.09; N, 2.88%. Found: C, 79.10, H, 8.11; N, 2.86%. FT–IR ($cm^{-1}$): 2915.2, 2848.8, 1721.8, 1609.3, 1592.9, 1511.8. $^1$H NMR ($CDCl_3$, 300 MHz): 8.599 (2H, s, PyH), 8.148 (2H, d, ArH), 7.590 (2H, d, ArH), 7.372 (2H, d, PyH), 7.337 (1H, s, CH=CH), 7.263 (2H, d, ArH), 7.013 (1H, s, CH=CH), 6.972 (2H, d, ArH), 4.040 (2H, t, $CH_2$), 1.270–1.845 (20H, m, $CH_2$), 0.884 (3H, t, $CH_3$).

## Acknowledgements

The authors acknowledge the National Nature Science Foundation of China (NNSFC) for financial support of this work.

## References


1 (*a*) P. Terech and R. G. Weiss, *Chem. Rev.*, 1997, **97**, 3133–3159; (*b*) J. H. Van Esch and B. L. Feringa, *Angew. Chem., Int. Ed.*, 2000, **112**, 2351–2354.

2 G. D. Rees and B. H. Robinson, *Adv. Mater.*, 1993, **5**, 608–619.

3 G. Haering and P. L. Luisi, *J. Phys. Chem.*, 1986, **90**, 5892–5895.

4 R. J. H. Hafkamp, P. A. Kokke and I. M. Danke, *J. Chem. Soc., Chem. Commun.*, 1997, **6**, 545–546.

5 (*a*) C. Y. Bao, R. Lu, M. Jin, P. C. Xue, C. H. Tan, Y. Y. Zhao and G. F. Liu, *Carbohydr. Res.*, 2004, **339**, 1311–1316; (*b*) C. Y. Bao, R. Lu, M. Jin, P. C. Xue, C. H. Tan, Y. Y. Zhao and G. F. Liu, *J. Nanosci. Nanotechnol.*, 2004, **4**, 1045–1051.

6 (*a*) G. John, J. H. Jung, H. Minamikawa, K. Yoshida and T. Shimizu, *Chem. Eur. J.*, 2002, **8**, 5494–5500; (*b*) A. Friggeri, O. Gronwald, K. J. C. van Bommel, S. Shinkai and D. N. Reinhoudt, *J. Am. Chem. Soc.*, 2002, **124**, 10754–10758.

7 J. H. Jung, M. Amaike, K. Nakashima and S. Shinkai, *J. Chem. Soc., Perkin Trans. 2*, 2001, 1938–1943.

8 M. Suzuki, M. Yumoto, M. Kimura, H. Shirai and K. Hanabusa, *Chem. Eur. J.*, 2003, **9**, 348–354.

9 M. Suzuki, T. Nigawara, M. Yumoto, M. Kimura, H. Shirai and K. Hanabusa, *Tetrahedron Lett.*, 2003, **44**, 6841–6843.

10 K. Yabuuchi, E. Marfo-Owusu and T. Kato, *Org. Biomol. Chem.*, 2003, **1**, 3464–3469.

11 (*a*) J. V. Esch, F. Schoonbeek, M. D. Looks, H. Kooijman, A. L. Spek, R. M. Kellogg and B. L. Feringa, *Chem. Eur. J.*, 1999, **5**(3), 937–950; (*b*) L. A. Estroff and A. de Hamilton, *Angew. Chem., Int. Ed.*, 2000, **39**(19), 3447–3450; (*c*) K. Hanabusa, K. Shimura, K. Hirose, M. Kimura and H. Shirai, *Chem. Lett.*, 1996, 885–886.

12 (*a*) Murata, M. Aokl, T. Suzuki, T. Harada, H. Kawabata, T. Komori, F. Ohseto, K. Ueda and S. Shinkai, *J. Am. Chem. Soc.*, 1994, **116**, 6664–6676; (*b*) K. Sugiyasu, N. Fujita, M. Takeuchi, S. Yamada and S. Shinkai, *Org. Biomol. Chem.*, 2003, **1**, 895–899.

13 (*a*) P. C. Xue, R. Lu, Y. Huang, M. Jin, C. H. Tan, C. Y. Bao, Z. M. Wang and Y. Y. Zhao, *Langmuir*, 2004, **20**, 6470–6475; (*b*) P. C. Xue, R. Lu, D. M. Li, M. Jin, C. Y. Bao, Y. Y. Zhao and Z. M. Wang, *Chem. Mater.*, 2004, **16**, 3702–3707.

14 Y. Lin and R. G. Weiss, *Macromolecules*, 1987, **20**, 414–417.

15 (*a*) K. Sugiyasu, N. Fujita, M. Takeuchi, S. Yamada and S. Shinkai, *Org. Biomol. Chem.*, 2003, **1**, 895–899; (*b*) J. H. Jung, Y. Ono and S. Shinkai, *Angew. Chem., Int. Ed.*, 2000, **39**(10), 1862–1865.

16 (*a*) S. Y. Ryu, S. Kim, J. Seo, Y. Kim, O. Kwon, D. Jang and S. Y. Park, *Chem. Commun.*, 2004, 70–71; (*b*) M. Ikeda, M. Takeuchi and S. Shinkai, *Chem. Commun.*, 2003, 1354–1355.

17 (*a*) M. Ayabe, T. Kishida, N. Fujita, K. Sada and S. Shinkai, *Org. Biomol. Chem.*, 2003, **1**, 2744–2747; (*b*) D. Bertheir, T. Buffeteau, J. Léger, R. Oda and I. Huc, *J. Am. Chem. Soc.*, 2002, **124**, 13486–13494; (*c*) M. G. George and R. G. Weiss, *Langmuir*, 2003, **19**, 1017–1025.

18 (*a*) A. R. Hirst, D. K. Smith, M. C. Friter, H. P. M. Geurts and A. C. Wright, *J. Am. Chem. Soc.*, 2003, **125**, 9010–9011; (*b*) K. S. Partridge, D. K. Smith, G. M. Dykes and P. T. McGrail, *Chem. Commun.*, 2001, 319–320; (*c*) K. Hanabusa, T. Miki, Y. Taguchi, T. Koyama and H. Shirai, *J. Chem., Soc., Chem. Commun.*, 1993, **18**, 1382–1383.

19 P. Babu, N. M. Sangeetha, P. Vijaykumar, U. Maitra, K. Rissanen and A. R. Raju, *Chem. Eur. J.*, 2003, **9**, 1922–1932.

20 M. Dukh, D. Šaman, J. KroulÍk, I. Černŷ, V. Pouzar, V. Krlā and P. Drašar, *Tetrahedron*, 2003, **59**, 4069–4076.

21 (*a*) D. W. Bruce, *Adv. Inorg. Chem.*, 2001, **52**, 151–152; (*b*) H. L. Nguyen, P. N. Horton, M. B. Hursthouse, A. C. Legon and D. W. Bruce, *J. Am. Chem. Soc.*, 2004, **126**, 16–17.

22 (*a*) R. Oda, I. Huc, M. Schmutz, S. J. Candau and F. C. MacKintosh, *Nature*, 1999, **399**, 566–569; (*b*) K. Sugiyasu, S. Tamaru, M Takeuchi, D. Berthier, I. Huc, R. Oda and S. Shinkai, *Chem. Commun.*, 2002, 1212–1213; (*c*) R. Oda, I. Huc and S. J. Candau, *Angew. Chem., Int. Ed.*, 1998, **37**, 2689–2691.

23 Y. Q. Tian, X. H. Xu, Y. Y. Zhao, X. Y. Tang and T. J. Li, *Liq. Cryst.*, 1997, **22**, 87–96, and the references therein.

24 N. Amanokura, K. Yoza, H. Shinmori, S. Shinkai and D. N. Reinhoudt, *J. Chem. Soc., Perkin Trans. 2*, 1998, 2585–2591.

25 (*a*) Y. C. Lin, B. Kachar and R. G. Weiss, *J. Am. Chem. Soc.*, 1989, **111**, 5542–5551; (*b*) L. Lu, T. M. Cocker, R. E. Bachman and R. G. Weiss, *Langmuir*, 2000, **16**, 20–34; (*c*) T. Sagawa, S. Fukugawa, T. Yamada and H. Ihara, *Langmuir*, 2002, **18**, 7223–7228.

26 S. Li, L. He, F. Xiong, Y. Li and G. Yang, *J. Phys. Chem. B*, 2004, **108**, 10887–10892.

27 (*a*) H. Yoshika and K. Nakatsu, *Chem. Phys. Lett.*, 1971, **11**, 255–258; (*b*) J. Bujadak, N. Iyi, J. Hrobáriková and T. Fujita, *J. Colloid Interface Sci.*, 2002, **247**, 494–503.